Minor-Groove Recognition of the Self-Complementary Duplex d(CGCGAATTCGCG)$_2$ by Hoechst 33258: A High-Field NMR Study†

John A. Parkinson,‡,§ Jill Barber,‡ Kenneth T. Douglas,*,‡ John Rosamond,∥ and Derek Sharples‡
Departments of Pharmacy and of Biochemistry and Molecular Biology, University of Manchester, Manchester M13 9PL, U.K.
Received February 27, 1990; Revised Manuscript Received July 2, 1990

ABSTRACT: The interaction of Hoechst 33258, a fluorescent DNA stain, has been studied by using the synthetic, self-complementary oligonucleotide duplex d(CGCGAATTCGCG)$_2$. Spectrofluorometric Scatchard analysis indicated that there was only a single class of binding site and that the 1:1 complex had a dissociation constant of $(3.47 \pm 0.1) \times 10^{-6}$ M at 25 °C. Spectroscopic titration by high-field ^{1}H NMR confirmed the 1:1 complex and by means of ID and 2D (NOESY, COSY) techniques the binding site was defined as the minor groove formed by the AATT stretch. Plentiful cross-peaks were measurable and resonance doubling occurred because of the lifting of the diad symmetry of the oligonucleotide on ligand binding. Many individual resonances of *both* strands of the DNA could be assigned for the complex because of these features, along with the occurrence of slow exchange on the NMR time scale. The results of this NMR spectroscopic solution study were compared with those of previous X-ray crystallographic studies of the same complex. From nuclear Overhauser effect data measured for the complex, a detailed three-dimensional model was constructed with the aid of molecular graphics.

It is now reasonable to consider routes to the development of synthetic molecules and tools for molecular biology based on DNA sequence recognition. Such molecules would allow a particular gene sequence (e.g., a cellular oncogene) to be occluded, and it is possible in principle to activate, suppress, or modify gene activity by appropriate, sequence-directed ligands. Even more exciting is to combine sequence recognition with a chemical DNA-scission mechanism as has been so elegantly demonstrated by using Fe–EDTA (Dreyer & Dervan, 1985), Cu–phenanthroline (Sigman, 1986), or porphyrins (Lown et al., 1986) as the cleaving agents. To underpin such approaches, and the development of new chemical cleavage systems for DNA (Reed & Douglas, 1989; John & Douglas, 1989), requires detailed knowledge of the structural features responsible for mutual recognition between ligand and target DNA. This study probes one aspect of such recognition.

There has been a considerable recent emphasis (Anderson et al., 1981; Baguley, 1982, Dervan, 1986, Goodsell & Dickerson, 1986; Wang, 1986; Zimmer & Wahnert, 1987; Kissinger et al., 1987; Neidle et al., 1987; Zakrzewska & Pullman, 1988) on studying the minor groove of B DNA as the binding site of relatively small ligands, e.g., netropsin, distamycin, berenil, Hoechst 33258 [for a review, see Baguley (1982)]. Footprinting and other studies have indicated an A + T selectivity for such minor-groove-directed ligands. Linked to this there have been several attempts, meeting with increasing success, to design molecules (Dervan, 1986; Goodsell & Dickerson, 1986; Kissinger et al., 1987; Zakrzewska & Pullman, 1988) (e.g., lexitropsins, isolexins) that can read a sequence from the minor groove. Consequently, detailed structural studies of minor-groove-binding ligands with B DNA are important to help define the recognition features in such partnerships.

Complementary to X-ray diffraction techniques, NMR has been used extensively to study DNA–drug interactions, mostly involving intercalating ligands. NMR studies of netropsin bound to several oligonucleotides in minor-groove AATT and TATA sequences have indicated several molecular contacts by nOe (nuclear Overhauser effect)[1] measurements (Patel & Shapiro, 1985, 1986a,b). Overall, the correspondence between solution and crystal structures is good. The bis-quaternary minor-groove ligand SN 6999 has been studied with the self-complementary d(CGATTAATGC)$_2$ by 1D and 2D NMR techniques and found to bind to two equivalent sites covering five A–T base pairs in the minor groove. In this case the lifetime of the drug–DNA complex is short relative to the NMR time scale, and fast exchange was detected for all but a few protons (Leupin et al., 1986). In both of these cases (netropsin and SN 6999) the two DNA strands of the duplex were found to be magnetically equivalent, indicating that there is (relatively) fast equilibrium between symmetrically equivalent, drug-binding sites on the duplex (Patel & Shapiro, 1985; Patel & Shapiro, 1986a,b; Leupin et al., 1986).

In a number of cases reported to date [for netropsin with d(GGAATTCC)$_2$ (Patel & Shapiro, 1986b), for (4*S*)-(+)-anthelvencen A with d(CGCAATTGCG)$_2$ (Lee et al., 1989), and for various lexitropsins with d(CGCAATTGCG)$_2$ (Lee et al., 1988b) and d(CATGGCCATG)$_2$ (Lee et al., 1988a)] individual strands could be detected by resonance doubling in the oligonucleotide–ligand complex.

Hoechst 33258 (**1**) binds preferentially in the minor groove of A-T rich regions of right-handed, double-stranded DNA (Ridler & Jennings, 1980) and is widely used as a fluorescent DNA stain. It binds to the duplex of the self-complementary oligonucleotide d(CGCGAATTCGCG), and two groups have crystallized the ligand–duplex complex and reported structural details of ligand binding (Pjura et al., 1987; Teng et al., 1988). The earlier crystal structure (Pjura et al., 1987) led to the proposal that **1** lies near one end of the AATT region with its

† We are grateful to the University of Manchester Research Fund for support (J.A.P.).
* Author to whom correspondence should be addressed.
‡ Department of Pharmacy.
§ Present address: Department of Chemistry, University of Edinburgh, West Mains Rd., Edinburgh, Scotland EH9 3JJ.
∥ Department of Biochemistry and Molecular Biology.

[1] Abbreviations: TSP, 3-(trimethylsilyl)propionic-2,2,3,3-d_4 acid, sodium salt; nOe, nuclear Overhauser effect; NOESY, two-dimensional nuclear Overhauser enhancement spectroscopy; COSY, two-dimensional homonuclear shift-correlated spectroscopy.

0006-2960/90/0429-10181$02.50/0

protonated piperazine ring protruding into, and binding in, the adjacent CG region, i.e., that binding occurs at the ATTC sequence. The other model (Teng et al., 1988) had **1** bound essentially centrally to the minor groove of the duplex occluding the AATT region only. In view of this discrepancy, we investigated the interaction of Hoechst 33258 with d-$(CGCGAATTCGCG)_2$ (for which the nomenclature to be used is given in **2**) by high-field ^1H NMR spectroscopy. A preliminary communication describing some aspects of the chemical shift data has appeared already (Parkinson et al., 1989). We now report the data more fully, together with an analysis of nOe connectivities in the drug–DNA complex.

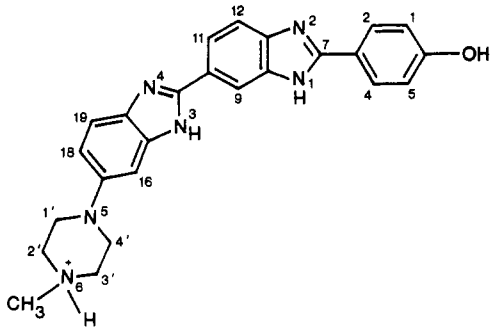

(1) Hoechst 33258

C^1 G^2 C^3 G^4 A^5 A^6 T^7 T^8 C^9 G^{10} C^{11} G^{12}

$G^{12'}C^{11'}G^{10'}C^{9'}$ $T^{6'}$ $T^{7'}$ $A^{6'}$ $A^{5'}$ $G^{4'}$ $C^{3'}$ $G^{2'}$ $C^{1'}$

(2) 12-Mer

Materials and Methods

(*a*) *Oligonucleotide Synthesis.* The oligonucleotide d-(CGCGAATTCGCG) was synthesized on an Applied Biosystems Model 381A solid-phase DNA synthesizer, using a 62-step automated phosphoramidite procedure. The support column (10 μmol) was supplied by Applied Biosystems, as were protected bases and solvents. On completion of the synthesis, the oligonucleotide was cleaved from the solid support and simultaneously deprotected by incubation at 55 °C in fresh, concentrated ammonium hydroxide solution (Applied Biosystems) for 12 h. The final volume of oligonucleotide solution was reduced to 2 mL by using a Speed-Vac concentrator. In this form the oligonucleotide was stored, deep frozen, until it was purified by reversed-phase HPLC as required.

(*b*) *Purification.* Hoechst 33258 was purchased from Aldrich U.K. and used without further purification. Before use its purity was assessed by HPLC (reversed-phase Rainin Dynamax C_{18} Microsorb analytical column, 0.1 M potassium dihydrogen phosphate (BDH, pH = 7.0)/methanol, 88/200). Under these conditions and with an eluent flow rate of 0.75 mL/min, Hoechst 33258 was found to have a retention time of 11 min.

The oligonucleotide was purified (in 15 aliquots) by reversed-phase HPLC, using a C_{18} column (Rainin Dynamax semipreparative, 250 × 10 mm) with 0.1 M ammonium acetate (pH = 7.0) and 0.1 M ammonium acetate/20% acetonitrile (pH = 7.0 as eluent and a Gilson dual-pump assembly to create an eluting gradient (flow rate, 3.0 mL/min; oligonucleotide retention time, 20 min). Oligonucleotide fractions were combined, desalted by using a Pharmacia (3 × 40 cm) column packed with Sephadex G-10 (water eluent), lyophilized, and stored frozen at −80 °C as the solid.

(*c*) *Spectrofluorometry.* The oligonucleotide [d-$(CGCGAATTCGCG)_2$] was dissolved in buffer (100 mM NaCl, 10 mM phosphate, pH = 7.0) to a final concentration of 100 μM. Aliquots of this solution (10 μL) were added to a solution (3 mL) of Hoechst 33258 in buffer (100 mM NaCl, 10 mM phosphate, pH = 7.0; ligand concentration = 3 μM). Fluorescence enhancement was measured by using a Perkin-Elmer spectrofluorometer. Site occupancy and the dissociation constant were computed for the complex by Scatchard analysis.

(*d*) *Sample Preparation for NMR Spectroscopy.* Oligonucleotide (17.2 mg) was divided into two equal portions, which were prepared for NMR spectroscopy in an identical manner. Each sample was dissolved in 400 μL of 99.8% D_2O (Aldrich) that contained 10 mM sodium phosphate (pH = 7.0), 100 mM sodium chloride, 1 mM TSP, and 0.1 mM NaN_3. The samples were lyophilized overnight and redissolved in 400 μL of 99.96% D_2O (Aldrich). Following further lyophilization, samples were dissolved in a final volume of 400 μL of D_2O (99.96%), to give a final oligonucleotide concentration of approximately 2.5 mM on the basis of weight and a molecular weight of 7150. The final pH of the sample was measured as 7.00 (uncorrected meter reading).

To form 1:1 and 0.5:1 molar ratio mixtures of Hoechst 33258 and the dodecamer, the Hoechst dye was prepared by dissolving Hoechst 33258·$5H_2O$·3HCl (5 mg) in approximately 100 μL of D_2O (99.96%). The sample pH was adjusted to 7.00 by gradual addition of concentrated NaOD (Aldrich). Complexes were formed by sequential titration, which was checked by NMR spectroscopy. The samples were transferred to Wilmad 528-PP NMR tubes, amber coated to protect the light-sensitive ligand.

(*e*) *NMR Experiments.* NMR spectra were recorded at 500.1 MHz (^1H) on a Bruker AM-500 NMR spectrometer equipped with a dedicated proton probehead, Aspect 3000 computer, and array processor. Probe temperature for most purposes was maintained at 303 ± 0.1 K, regulated by using the spectrometer's variable-temperature unit.

Two-dimensional NOESY and chemical-exchange NMR spectra (Jeener et al., 1979; Macura et al., 1981) of nonexchangeable protons were collected on a nonspinning sample, with quadrature detection, into 2048 complex data points for 360 t_1 increments in the phase-sensitive (TPPI) mode (Marion & Wüthrich, 1983); 64 transients were acquired for each t_1 increment with a recycle delay of 2 s between acquisitions. Data were acquired with a spectral width of 5 kHz giving a final digital resolution of 2.5 Hz/point by using a 90° pulse length of 10.4 μs. The residual *H*OD resonance was suppressed by continual irradiation during the mixing time and the recycle delay. Data were zero-filled in F1 before apodization, which was applied in both time domains by using a $\pi/2$ shifted sine-bell window function. Fourier transformation of the resulting data was carried out with phase correction in the F2 frequency domain only. A mixing time of 350 ms was randomly varied by 6% over the period of the experiment.

Two-dimensional NOESY spectra of exchangeable protons (Rajagopal et al., 1988) were acquired by using a sample dissolved in 90% H_2O/10% D_2O. The carrier frequency was set to the solvent resonance frequency and made phase coherent with the decoupler channel. Data were collected on a nonspinning sample, with quadrature detection into 2048 complex data points for 256 t_1 increments in the phase-sensitive (TPPI) mode (Marion & Wüthrich, 1983) over a sweep width of 20 ppm (10 kHz); 96 transients were acquired for each t_1 increment with a recycle delay of 1.8 s between scans. The solvent resonance was suppressed by continual irradiation

during the recycle delay and the mixing time. Data were zero filled in F1 before apodization. Fourier transformation was carried out by application of a $\pi/4$ shifted, squared sine-bell window function in both dimensions. A mixing time of 300 ms was randomly varied by 8% over the period of the experiment.

Two-dimensional COSY (Nagayama et al., 1980; Aue et al., 1976) data were collected with quadrature detection into 1024 complex data points for 256 t_1 increments in the magnitude mode; 64 transients were acquired for each t_1 increment with a recycle delay of 2 s between acquisitions. Data were acquired with a spectral width of 5 kHz, giving an F2 digital resolution of 4.87 Hz/point. Data were zero filled once in F2 and Fourier transformed in both dimensions with an unshifted sine-bell window function. The residual *H*OD resonance was suppressed by continual irradiation during the pulse sequence. The decoupler was gated off during the acquisition period.

One-dimensional NMR spectra of samples dissolved in 90% H_2O were obtained by using a binomial pulse sequence for water suppression (Hore, 1983a,b). Data were acquired with a spectral width of 10 kHz giving a final digital resolution of 0.6 Hz/point. The transmitter power was attenuated with a tunable notch filter to give a 90° pulse length of approximately 40 μs. A $1\bar{3}3\bar{1}$ pulse scheme (Hore, 1983a,b) was used for attenuation of the H_2O resonance. Data were processed by using 2-Hz line broadening and baseline corrected by using a standard baseline correction procedure.

(*f*) *Molecular Modeling.* Molecular modeling was carried out on a Silicon Graphics IRIS 4D/240GTX hardware system, using the Polygen QUANTA and CHARMM software.

Results

1. Fluorometric Scatchard Analysis and Binding Constants. In general, spectrofluorometric Scatchard analysis of ligand binding to macromolecules is carried out by the addition of aliquots of ligand to a fixed concentration of macromolecule (Segel, 1975). In this study, however, oligonucleotide was added to a fixed quantity of ligand since the latter was more readily available. When oligonucleotide was first added, all sites in the oligonucleotide became occupied by excess ligand. At any oligonucleotide concentration, the fraction of oligonucleotide bound was determined from a standard plot of relative fluorescence versus total oligonucleotide concentration.

The plots of ($[\text{oligo}]_{\text{bound}}/[\text{Hoechst}]_{\text{total}}[\text{oligo}]_{\text{total}}$) versus ($[\text{oligo}]_{\text{bound}}/[\text{Hoechst}]_{\text{total}}$) were linear (Figure 1) and gave a dissociation constant (K_d) of $(3.47 \pm 0.01) \times 10^{-6}$ M, showing that the ligand binds tightly to DNA. From the intercept of Figure 1, a site occupancy of one ligand per DNA molecule was found. From such data and the linearity of Figure 1, a 1:1 complex was anticipated to form on mixing equimolar quantities of the ligand (Hoechst 33258) and the oligonucleotide $[d(CGCGAATTCGCG)]_2$.

2. NMR Titration of Oligonucleotide with Ligand. General Characterization of the Binding of Hoechst 33258 to DNA. Small aliquots of a solution of Hoechst 33258 were added to a solution of the oligonucleotide in D_2O to give 0:1, 0.25:1, 0.5:1, 0.75:1, and 1:1 ligand to oligonucleotide molar ratios. The ^1H NMR spectrum (500 MHz) of each sample was recorded (not shown). At molar ratios of 0.25:1, 0.5:1, and 0.75:1 distinct signals from the free and bound oligonucleotide were observed in the same spectrum, indicating slow exchange on the NMR timescale, consistent with a K_d of 3.47×10^{-6} M. An interesting characteristic of the spectrum of the complex is the appearance of many "doubled" resonances. This doubling is the result of the two oligonucleotide strands of the duplex, previously identical in the unbound form, becoming

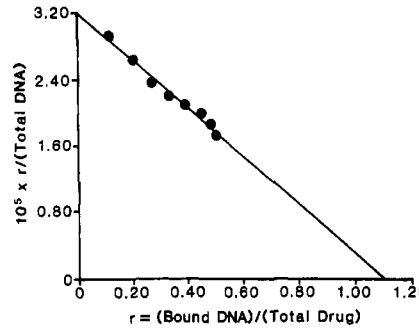

FIGURE 1: Scatchard plot of data derived from the spectrofluorometric titration of Hoechst 33258 with the oligonucleotide d-(CGCGAATTCGCG). Points are experimental; the line is by least-squares linear regression analysis using the following equation, where $r = [\text{DNA}]_{\text{bound}}/[\text{drug}]_{\text{total}}$ and $[A] = [\text{DNA}]_{\text{bound}} + [\text{DNA}]_{\text{free}}$:

$$\frac{r}{[A]} = \frac{1 - r}{(3.47 \pm 0.01) \times 10^{-6}}$$

(magnetically) nonidentical in the complex because of the tight binding of the unsymmetrical ligand. Binding must be tight for such divergence in chain identity to be manifest. The doubling is particularly evident toward the center of the complex. For example, when the experiment was repeated with 90% H_2O, 10% D_2O as the solvent, the A-T imino hydrogen resonances (δ 14.1–13.7) were both doubled to give four lines, whereas only one of the three G-C imino resonances (δ 13.1–12.8) was doubled. This is consistent with a complex in which 1 binds in the central region of the oligonucleotide, with effects extending into a GC region. Hence, even at this very superficial level, the evidence favors ligand binding in the GAATTC portion of the oligonucleotide, $d-(CGCGAATTCGCG)_2$.

3. Assignment of Nonexchangeable ^1H NMR Resonances. (*a*) *Details of Assignment.* To define more precisely the binding site of **1** with $d(CGCGAATTCGCG)_2$, the ^1H NMR spectra of free oligonucleotide and free **1** had first to be assigned fully, to identify which resonances corresponded to specific protons in the complex. This will be described in detail elsewhere but depends essentially on two approaches. Figure 2 shows three types of spectra. Spectrum a shows the "fingerprint" C1′H to aromatic cross-peak region of the NOESY spectrum of the free DNA. Spectrum b shows the aromatic to aromatic cross-peak region of the 2D exchange spectrum acquired on a sample of 0.5:1 ligand:oligonucleotide. Spectrum c shows the NOESY fingerprint region of the complex. The chemical exchange spectrum b acts as a bridge between the (assigned) spectrum of the free oligonucleotide (Hare et al., 1983) and the spectrum of the 1:1 complex. For example, T^8C6H resonates at about δ 7.35 in the free oligonucleotide and correlates with two signals at δ 6.91 and δ 6.96 in the chemical exchange spectrum (Figure 2b). These two signals are in turn correlated to the two $T^7C1'H$ signals by using the NOESY spectrum (Figure 2c). A number of cross-peaks in both the complex and free oligonucleotide fingerprint regions are in almost identical positions. The cross-peak labeled x in Figure 2a had been assigned previously as relating the C^1C1' and C^1C6 hydrogen resonances. This relationship appears as a NOESY cross-peak in the same position in the spectrum of the complex and is labeled x in Figure 2c.

Figure 3 shows the same portion of the NOESY spectrum as Figure 2c, but illustrating the well-established sequential mapping approach to the assignments of spectra of B DNA structures (Patel et al., 1987; Reid, 1987). This approach depends on the proximity of a sugar 1′-hydrogen to the aro-

Table I: Assignment of the ^{1}H NMR Spectrum of the 1:1 Complex Formed between Hoechst 33258 and d(CGCGAATTCGCG)$_2$[a]

	C8H	C6H	CH_3	C5H	C1′H	C2′H	C2″H	C3′H	C4′H	C5′H	C3′H
					Strand A						
C^1		7.61		5.85	5.72	1.94	2.39	4.65	4.06	3.71	3.71
G^2	7.93				5.835	2.63	2.70	4.92	4.35	3.095	3.98
C_3		7.23		5.33	5.65	1.70	2.19	4.76	4.13	3.75	3.75
G^4	7.84				5.53	2.62	2.81	4.98	4.37	nd	nd
A^5	8.15				6.09	2.72	2.85	5.05	4.50	4.24	4.24
A^6	8.07				6.19	2.64	2.76	5.02	4.50	nd	nd
T^7		6.98	1.34		5.31	1.62	2.08	4.42	nd	nd	nd
T^8		6.94	1.43		5.08	1.62	2.13	4.42	nd	nd	nd
C^9		7.05		5.32	5.19	1.62	2.03	4.60	3.85	3.35	3.21
G^{10}	7.80				5.80	2.58	2.68	5.10	4.39	3.97	3.87
C^{11}		7.34		5.37	5.74	1.91	2.35	4.78	4.19	4.16	4.16
G^{12}	7.94				6.13	2.38	2.62	4.66	4.19	4.09	4.09
					Strand B						
$C^{1'}$		7.61		5.85	5.72	1.94	2.39	4.65	4.06	3.71	3.71
$G^{2'}$	7.93				5.835	2.63	2.70	4.92	4.35	4.095	3.98
$C^{3'}$		7.27		5.33	5.525	1.85	2.27	4.76	4.13	3.75	3.75
$G^{4'}$	7.82				5.05	2.62	2.81	4.98	nd	nd	nd
A^5	8.15				5.80	2.63	2.89	4.92	4.34	nd	nd
$A^{6'}$	8.28				5.815	2.61	2.77	4.74	nd	nd	nd
$T^{7'}$		6.80	1.18		5.12	1.54	2.06	4.39	nd	nd	nd
$T^{8'}$		6.91	1.40		4.97	1.60	2.13	nd	nd	nd	nd
$C^{9'}$		7.36		5.49	5.27	2.04	2.22	4.55	nd	nd	nd
$G^{10'}$	7.89				5.87	2.58	2.68	4.96	4.39	3.97	3.87
$C^{11'}$		7.34		5.43	5.74	1.91	2.35	4.78	4.19	4.16	4.16
$G^{12'}$	7.94				6.13	2.38	2.62	4.66	4.19	4.09	4.09

[a] Strands A and B are treated separately. The assignment of 4′, 5′, and 5″ hydrogens is limited due to overcrowding in the 2D NOESY and COSY data sets. Assignments that currently cannot be defined are replaced by nd (assignment *n*ot *d*efined).

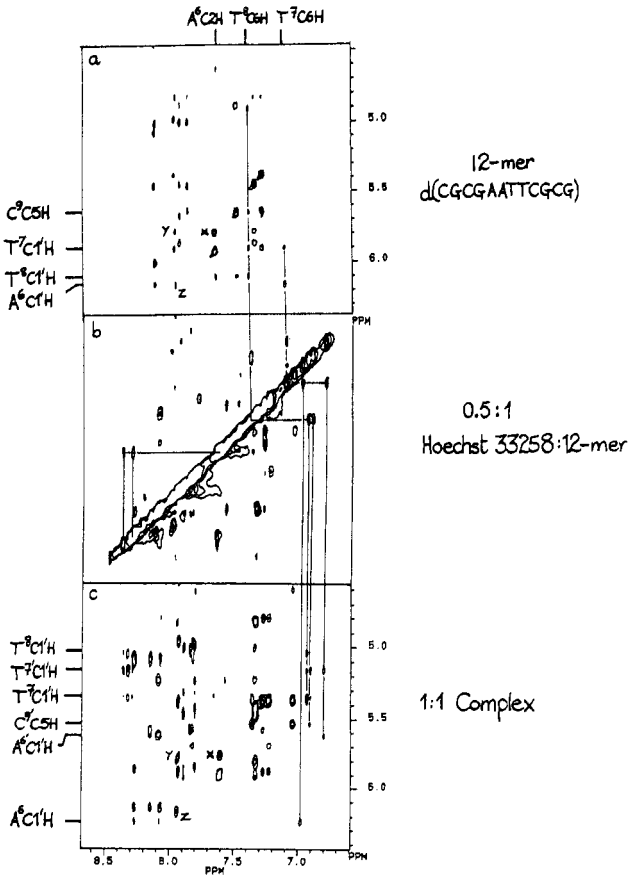

FIGURE 2: Use of 2D exchange spectroscopy to identify resonance assignments in the ^{1}H spectrum of the 1:1 complex of Hoechst 33258 with d(CGCGAATTCGCG)$_2$. (a) Fingerprint region of the 2D NOESY spectrum of free 12-mer duplex in D_2O at 303 K with a mixing time of 200 ms. (b) Aromatic to aromatic cross-peak region of the 2D exchange spectrum of 0.5:1 Hoechst 33258–12-mer at 303 K with a mixing time of 150 ms in D_2O. (c) Fingerprint region of the 2D NOESY spectrum of a 1:1 complex of Hoechst 33258–12-mer in D_2O at 303 K with a mixing time of 250 ms. See text for details.

matic hydrogen on the same residue and to one on the adjacent residue in the 3′-direction. Thus, $C^1C1'H$ gives cross-peaks to C^1C6H and to G^2C8H, which connects in turn to $G^2C1'H$, and so on. Even at 500 MHz there is spectral crowding and the use of two independent approaches allows the assignments to be made with confidence. By use of methods similar to those outlined for the fingerprint region of the NOESY spectrum, the sequential resonance assignments were extended from C8/C6 and C1′ hydrogens to C2′, C2″, and C3′ hydrogens where possible. Confirmation of the scalar couplings was made by using two-dimensional COSY spectroscopy (data not shown). The selective assignments for the ^{1}H NMR resonances of the ligand-bound oligonucleotide nonexchangeable hydrogens are shown in Table I.

(*b*) *Chemical Shift Measurements.* To determine more closely the position of the ligand within the GAATTC region of the oligonucleotide, chemical shift differences shifts of those same protons in the free oligonucleotide were measured. These differences, together with those for C2′, C2″, C3′, and aromatic hydrogens, are represented graphically in Figure 4, as plots of chemical shift difference versus position of the base or sugar in the oligonucleotide chain. All of these graphs show some element of symmetry about the diad center of the duplex, although none of them is expected to be perfectly symmetrical because of the unsymmetrical nature of the bound ligand. (There is further analysis of this in the Discussion.) This provides evidence for gross symmetry about the AATT center and further refines the ligand binding site within the six central base pairs to the *AATT* region. Deeper refinement still is based on intermolecular nOes observed between the ligand and oligonucleotide and is explained under Intermolecular Contacts in the Complex.

4. Assignment of Exchangeable-Hydrogen NMR Resonances. Sequential resonance assignment of the labile protons of the complex was made by using a NOESY spectrum acquired with presaturation of the solvent (H_2O) NOESY resonance during the recycle delay and mixing time. The 2D

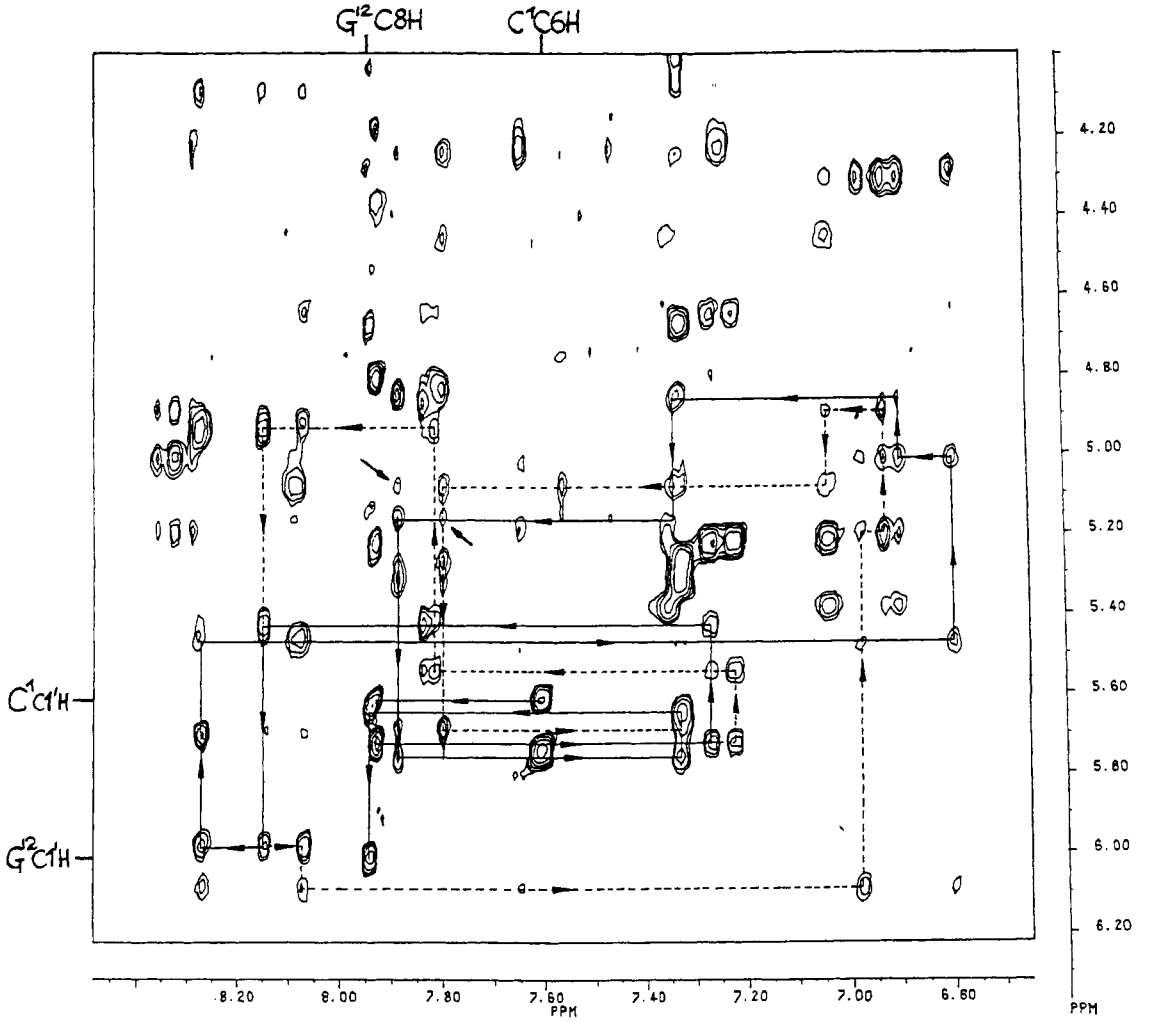

FIGURE 3: Fingerprint region of the 2D NOESY spectrum of the Hoechst 33258–12-mer complex. The cross-peaks between C^1 C1′H and C^1 C6H resonances and between G^{12} C1′H and G^{12} C8H resonances are indicated. Sequential assignment mapping for both strands of the oligonucleotide duplex is shown from the 5′- to the 3′-end of each strand. Where the strands differ in identity, the mapping of one of the strands is continued with a broken rather than a solid line. Exchange cross-peaks are indicated by arrows.

NOESY spectrum was acquired at 303 K with a mixing time of 300 ms. Exchange between some of the labile protons and the solvent is slow, as shown by the appearance of cross-peaks between exchangeable and nonexchangeable hydrogens and, even more convincingly, between pairs of exchangeable hydrogens. Figure 5 shows part of this spectrum. The nonexchangeable adenine C2 hydrogen resonances were assigned sequentially, as shown in Figure 5, on the basis of large interstrand nOes with the thymidine N3H of the same Watson–Crick base pair. In the same way, amino hydrogens [A C6H(1), A C6H(2), C C4H(1), and C C4H(2)] were assigned by reference to similar interstrand nOes with the thymidine N3H and guanine N1H, respectively, of the same Watson–Crick base pairs (see Figure 6). The additional resonances between δ 11.00 and 12.50 were assumed to be benzimidazole NH hydrogens from the ligand molecule. These were assigned together with the nonexchangeable hydrogen resonances of the ligand. Table II shows the assignments of the oligonucleotide exchangeable resonances and the nonexchangeable adenine C2H resonances. The nonexchangeable hydrogen resonances of Hoechst 33258 in the complex are shown in Figure 7.

5. Intermolecular Contacts in the Complex. On the basis of sequence-specific resonance assignments, the intermolecular contacts between d(CGCGAATTCGCG)$_2$ and **1** were probed by 2D NOESY spectroscopy. It has already been established that **1** binds in the AATT region of the 12-mer. As a general rule, chemical shifts of the nonexchangeable hydrogen resonances (especially those related to T residues) on both strands were found to move toward lower frequency (more shielded). On the other hand, chemical shifts of exchangeable (especially amino) and adenine C2 hydrogen resonances became more deshielded. In qualitative terms, these observations can provide some of the details of ligand binding. In effect, the deshielding experienced by C2 and imino hydrogens is the result of an aromatic ring lying nearby, such that the oligonucleotide hydrogen atoms are in the negative field of the ring (Figure 8a). On the other hand, the shielding experienced by TC1′ hydrogens arises from positive diamagnetic anisotropy, since they are perpendicular to the plane of the ligand molecule, see Figure 8b. These details are clear evidence for **1** binding in the minor groove of d(CGCGAATTCGCG)$_2$, explained more fully under Discussion.

The much larger chemical shift changes observed for T C1′ hydrogens than for A C1′ hydrogens could indicate that the ends of the ligand associate more closely with the T than the A regions of both strands. Thus, the molecule may not be centrally disposed down the central region of the minor groove.

These data were used to derive more direct information on the proximity of individual hydrogens to one another, between **1** and d(CGCGAATTCGCG)$_2$. Table III presents a list of all assigned intermolecular nOes, which are summarized diagrammatically (Figure 9). The overall conclusion is that

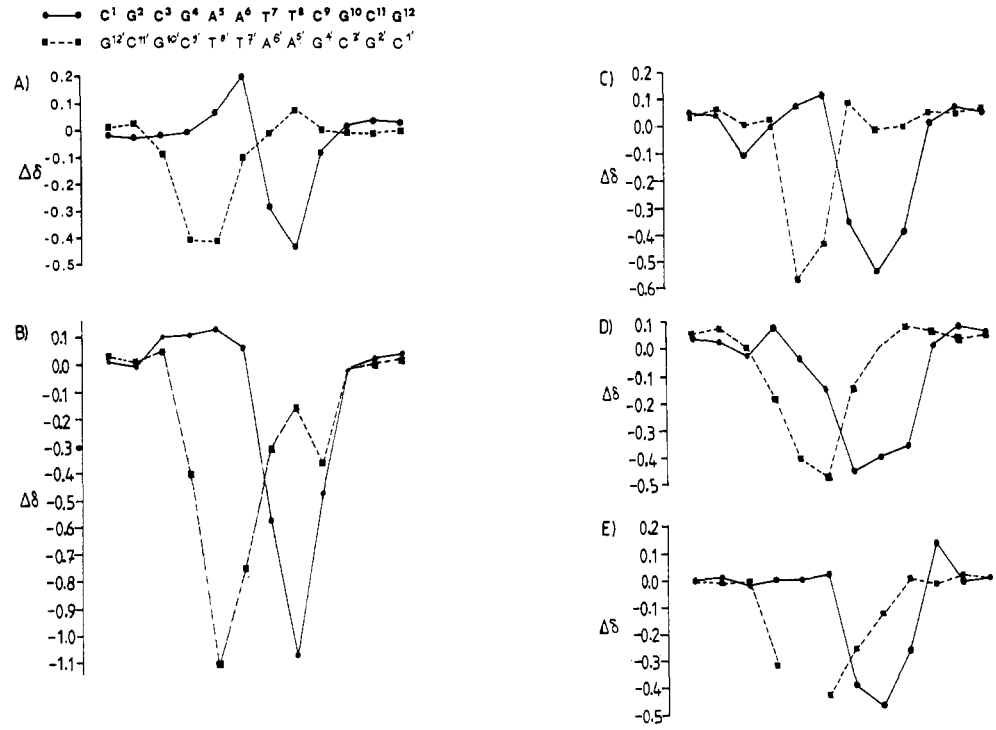

FIGURE 4: Chemical shift differences for some oligonucleotide resonances in the 1:1 complex with Hoechst 33258 as a function of position in the chain. δ is the difference between the chemical shift of a particular hydrogen resonance from the oligonucleotide of the complex and the chemical shift of the resonance from the same hydrogen in the free oligonucleotide. Each strand in the complex has a different identity. Thus strand A is represented by (—) and is related to $C^1G^2C^3G^4A^5A^6T^7T^8C^9G^{10}C^{11}G^{12}$. Strand B is represented by (---) and is related to $G^{12'}C^{11'}G^{10'}C^{9'}T^{8'}T^{7'}A^{6'}A^{5'}G^{4'}C^{3'}G^{2'}C^{1'}$. (A) Aromatic C6H and C8H resonances; (B) sugar C1'H resonances; (C) sugar C2'H resonances; (D) sugar C2''H resonances; (E) sugar C3'H resonances.

Table II: Assignment of Nonexchangeable C2H and Exchangeable Amino and Imino Hydrogen Resonances of Hoechst 33258 Bound Oligonucleotide d(CGCGAATTCGCG)$_2$, in the ^{1}H NMR Spectrum Recorded at 500 MHz

	C2H	amino CH4(1)	amino CH4(2)	imino CH1	imino CH3
			Strand A		
C^1					
G^2				13.07	
C^3		6.45	8.38		
G^4				12.98	
A^5	7.475				
A^6	8.29				
T^7					14.08
T^8					13.63
C^9		6.49	8.40		
G^{10}				12.88	
C^{11}		6.56	8.44		
G^{12}					
			Strand B		
$C^{1'}$					
$G^{2'}$				13.07	
$C^{3'}$		6.45	8.38		
$G^{4'}$				12.98	
$A^{5'}$	7.56				
$A^{6'}$	8.34				
$T^{7'}$					13.96
$T^{8'}$					13.71
$C^{9'}$		6.73	8.45		
$G^{10'}$				12.88	
$C^{11'}$		6.62	8.47		
$G^{12'}$					

Table III: Intermolecular nOes Deduced from 2D NOESY Spectra for the Hoechst 33258/d(CGCGAATTCGCG)$_2$ Complex[a]

strand A	strand B
A^5 C2H to Hoechst CH_3 (m)	$C^{9'}$ C1'H to Hoechst CH_3 (s)
A^5 C2H to Hoechst piperazine CH_2's (m)	$C^{9'}$ C1'H to Hoechst piperazine (m)
A^5 C2H to Hoechst H16	$T^{8'}$ C1'H to Hoechst piperazine (m)
A^6 C2H to Hoechst piperazine CH_2's	$T^{7'}$ C1'H to Hoechst H9 (m)
A^6 C2H to Hoechst H19 (s)	$T^{7'}$ C2''H to Hoechst H9 (s)
A^6 C2H to Hoechst H16 (l)	$C^{6'}$ C2H to Hoechst piperazine
A^6 C2H to Hoechst N3H (m)	$A^{6'}$ C2H to Hoechst H16
T^7 C1'H to Hoechst H9 (s)	$A^{6'}$ C2H to Hoechst N1H (m)
T^8 C1'H to Hoechst H9 (s)	$A^{6'}$ C2H to Hoechst 2 or 4 (m)
C^9 C1'H to Hoechst 2 or 4 (m)	$A^{6'}$ C2H to Hoechst 1 or 5 (s)
C^9 C2''H to Hoechst 2 or 4 (s)	$A^{5'}$ C2H to Hoechst 2 or 4 (l)
G^{10} C8H to Hoechst 1 or 5	$A^{5'}$ C2H to Hoechst 1 or 5 (l)

[a] The magnitude of the nOe concerned is indicated qualitatively by s (small), m (medium), or l (large).

1 binds in the minor groove of the AATT region of the oligonucleotide d(CGCGAATTCGCG)$_2$. This could be in a skewed fashion, which allows the ends of the ligand to be more closely associated with one DNA strand rather than being symmetrically disposed between the two strands of DNA, i.e., the drug could "cross" the minor groove. Graphical modeling studies are under way to refine this structure and to fit more precisely the nOe data derived from intermolecular contacts between **1** and d(CGCGAATTCGCG)$_2$. However, a model consistent with the nOe data has been built and energy minimized. Figure 10, a view of this model, shows how the drug fits extremely snugly into the minor groove.

Discussion

The interaction between sonicated calf thymus DNA and Hoechst 33258 has been shown to be characterized by two binding processes, differing in binding constant by 1–2 orders of magnitude. The tighter binding mode involves binding of a low number of dye molecules on the outside of the double helix with their long axis at 45° to the helix axis. The tight-binding process (with binding constant $\sim 10^6$–10^7 M^{-1}) is important at Hoechst 33258:DNA phosphate ratios of less than approximately 0.05:0.20. The weaker interaction (binding

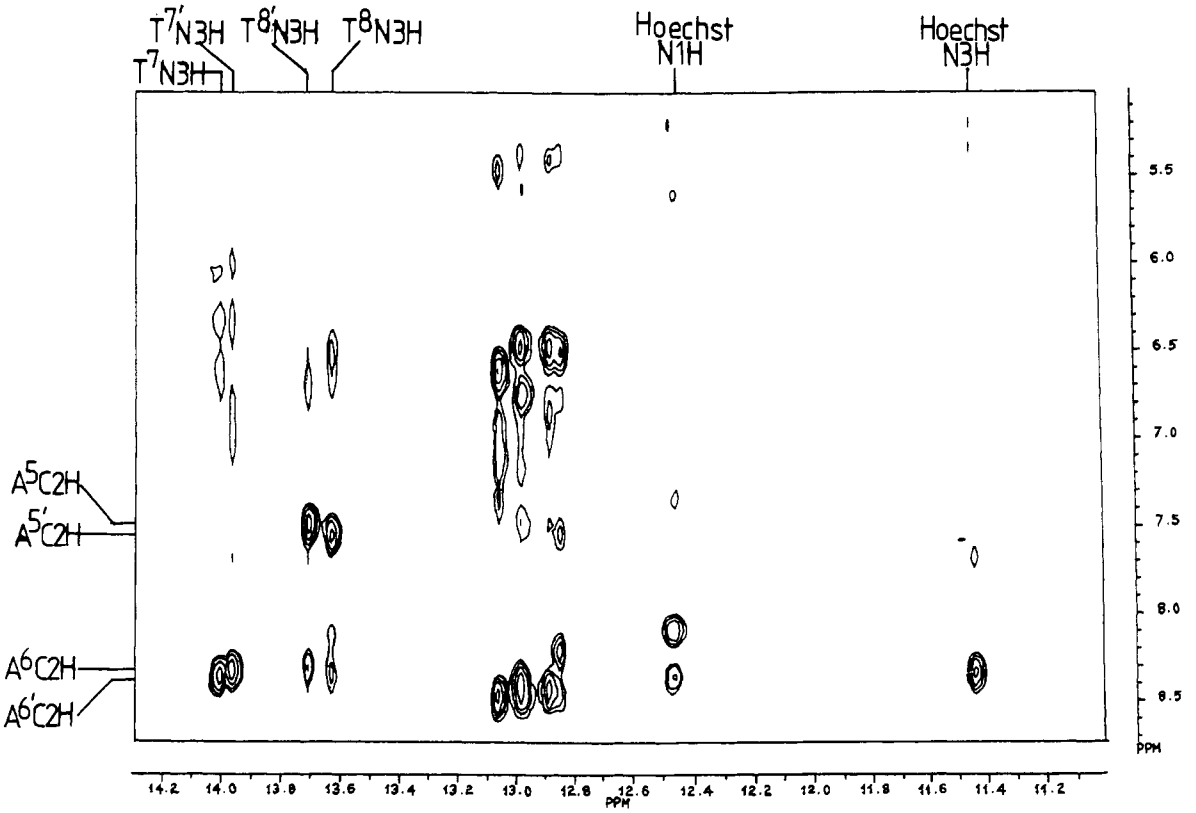

FIGURE 5: NOESY spectrum of the 1:1 Hoechst 33258–12-mer complex in H_2O (see text for details); expansion showing assignments of cross-peaks relating some exchangeable imino hydrogen resonances to nonexchangeable C2 hydrogen resonances. In addition, intermolecular contacts are observed by the presence of NOE cross-peaks between Hoechst 33258 N1 and N3 hydrogens and oligonucleotide $A^{6'}$ C2 and A^6 C2 hydrogens. Additional cross-peaks (not labeled) relate amino hydrogen resonances to imino hydrogen resonances.

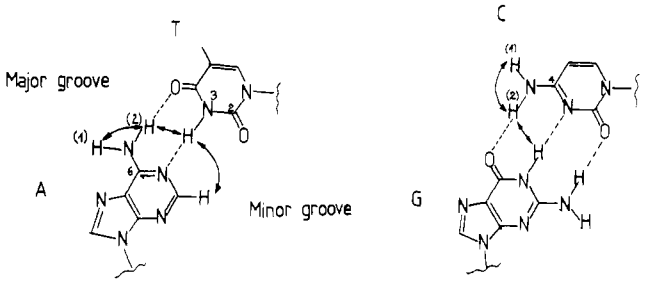

FIGURE 6: Spatial relationship between amino and imino hydrogen of both A-T and G-C base pairs with arrows indicating expected nOe connectivities.

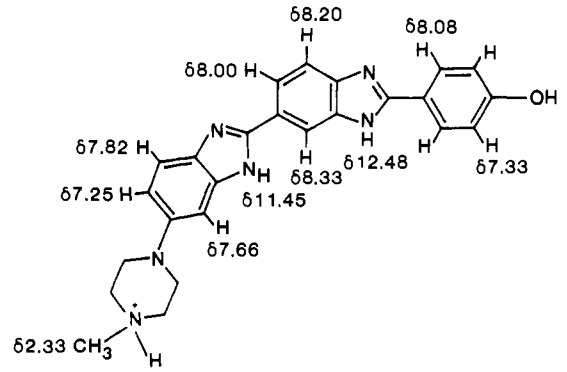

FIGURE 7: Assignments of hydrogens in the Hoechst 33258 molecule when bound to the oligonucleotide $d(CGCGAATTCGCG)_2$.

constant 10^4–10^5 M^{-1}) also involves external binding of this ligand but is only important at higher ligand:phosphate ratios (Bontemps et al., 1975; Stokke & Steen, 1985). All indications are that the tight binding occurs in the minor groove to A,T-rich sequences. Evidence for this is summarized by Pjura et

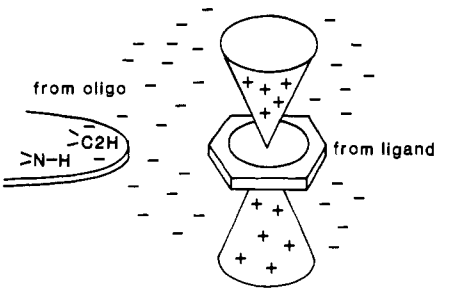

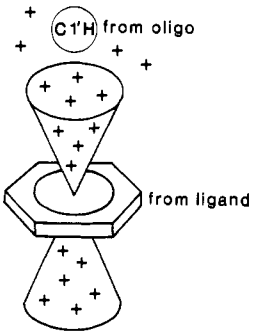

FIGURE 8: Pictorial representation of the local fields experienced by both (top) C2 imino and (bottom) C1′ hydrogens on the oligonucleotide when aromatic rings from the minor-groove-binding ligand Hoechst 33258 bind in close proximity to these hydrogens. Since the C1′ hydrogens sit above the shielding regions of a ring placed in the minor groove, the 1′H resonances shift to lower frequency (more shielded). On the contrary, C2″ and imino hydrogens sit in the deshielding region parallel to the plane of the aromatic ring in the minor groove. Hence C2H and NH resonances shift to higher frequency (more deshielded).

al. (1987). In both of the X-ray diffraction studies which have been reported on crystals of Hoechst 33258 with d-

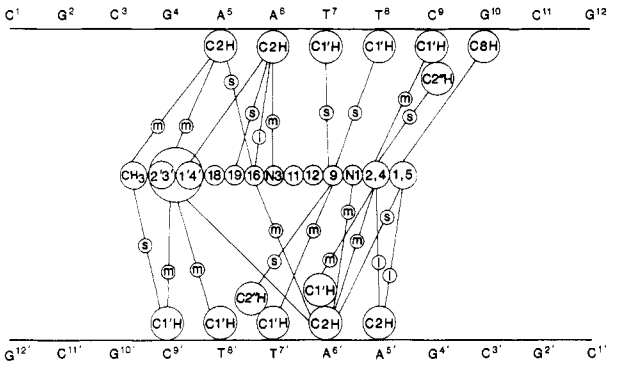

FIGURE 9: Diagrammatic presentation of observed intermolecular nOe detailed in Table III.

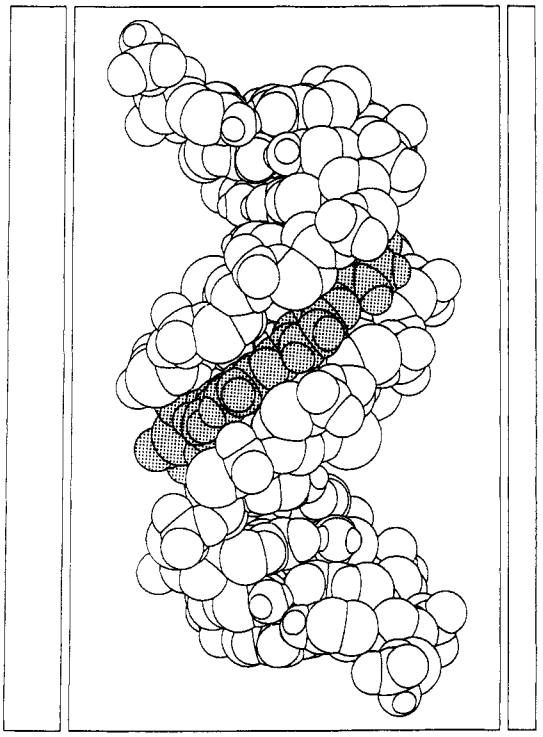

FIGURE 10: Picture of a model of Hoechst 33258 (shaded spheres) bound in the minor groove of a B DNA 12-mer of sequence [d-(CGCGAATTCGCG)]$_2$. The ligand is seen bound at the AATT site of the DNA structure.

(CGCGAATTCGCG)$_2$ the dye was located in the minor groove (Pjura et al., 1987; Teng et al., 1988).

We find that binding of Hoechst 33258 to the synthetic oligonucleotide d(CGCGAATTCGCG)$_2$ is well-described by a linear Scatchard plot with a drug:oligonucleotide duplex stoichiometry of 1:1 and a binding constant of 2.88×10^5 M^{-1}. There is no indication of two classes of binding site, as reported for "native" DNA (Bontemps et al., 1975; Stokke & Steen, 1985). Further evidence of complexation comes from the 1D NMR spectral titration. Detailed evidence of complexation and the nature of the ligand-binding site came from 2D NOESY studies, dicussed later.

Although the assignment of the ^{1}H NMR spectrum of the Hoechst 33258–12-mer complex is not complete, particularly in regard to the piperazine ring of the dye, enough detailed information is available from the data for it to be possible to draw a number of firm conclusions.

Structure of Bound DNA. DNA in the complex has gross structural characteristics similar to those of the free DNA in solution. The occurrence of imino hydrogen resonances at their characteristic chemical shifts for imino hydrogens in DNA base pairs and the many interstrand cross-peaks, especially those between exchangeable amino or imino and nonexchangeable adenine C2 hydrogen resonances, in the NOESY data set, show the DNA to be duplex along its entire length, with the exception of the C^1-G^{12} base pair. This is frayed, as evidenced by the absence of an imino hydrogen resonance for this base pair in the high-frequency region of the NMR spectrum. A similar effect has been noted for the binding of a lexitropsin to d(CGCAATTGCC)$_2$ (Lee et al., 1988b).

In addition, base pairing along the length of the oligonucleotide is not disrupted by the tight binding of the Hoechst 33258 ligand. The chirality of the double helix is right handed on the basis of well-established rules for the assignment of such oligonucleotides. Thus, the Hoechst 33258 bound oligonucleotide has largely characteristic B-type features.

At a more detailed level, however, perturbations of the double-helical structure are evident. Distortions in the structure of the central GAATTC region of the oligonucleotide are clearly seen. Some indication of this can be obtained from Figure 10.

(*i*) *Resonance Doubling.* In the imino region of the ^{1}H NMR spectrum, a number of the resonances are doubled, viz., for G^4-C^9, A^5-T^8, and A^6-T^7 base pairs. This doubling is a reflection of the tight binding of a nonsymmetrical ligand in the central GAATTC region of the 12-mer. Our analysis of the data suggests that the dye binds centrally across the AATT region. Perturbation of structure immediately adjacent to both 5′- and 3′-ends of this region (reflected in the G^4-C^9 imino resonance doubling) is a result of the length of the Hoechst 33258 molecule. Molecular modeling of the complex (based on observed nOe contacts, see below) has shown that when the dye is bound centrally to the AATT region, the ends of the dye protrude beyond the planes of the A^5-T^8 base pairs into the G^4-C^9 base pair regions.

The doubling of many resonances of nonexchangeable hydrogens is a reflection of the same feature, viz., tight binding of the unsymmetrical dye to the oligonucleotide, lifting the diad symmetry. Although it is possible that this resonance doubling could be the result of two binding sites, we shall show that Hoechst 33258 only binds to one site on this oligonucleotide duplex.

(*ii*) *Pattern of Intramolecular nOes.* The assignment "walk" shown in Figure 3 clearly reveals the nonequivalent strand nature of the double helix in the complex. Since the dye binds in the minor groove, one would expect most structural distortion in the minor-groove region. However, distortions in the DNA are clearly visible by the dramatic changes in chemical shift observed by the thymine C6 hydrogen resonances (see Figure 2). Since these hydrogens protrude into the major groove, it is clear that there is perturbation of the DNA structure in the central AATT region of the oligonucleotide in the presence of the Hoechst dye. The data could be a reflection of a combination of different types of structural alteration relating to base pair tilt, propeller twisting, helical twist and rise, etc. At this stage, we have not undertaken a detailed analysis of these alterations.

Gross Location of the Binding Site for Hoechst 33258 on d(CGCGAATTCGCG). Both chemical shift evidence and intermolecular nOes locate the ligand at the AATT region of the oligonucleotide.

(*i*) *Evidence from Chemical Shift Difference Measurements.* Figure 4 reveals that the biggest change in chemical shift for any single type of proton in the double helix of d-(CGCGAATTCGCG) is for the 1′-hydrogens when Hoechst 33258 is bound. Smaller but not inconsiderable changes are

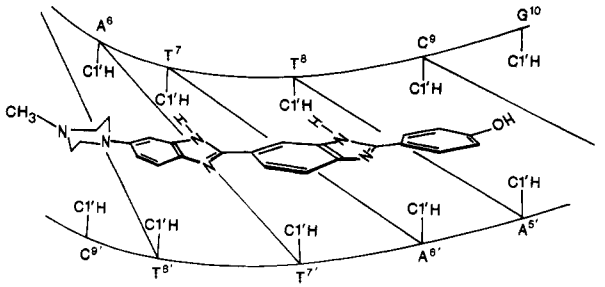

FIGURE 11: Location of 1'-hydrogens at the binding site with respect to the position of the aromatic moieties of the Hoechst dye when bound at the AATT site in the 12-mer. The chemical shift diagrams of Figure 4 can be fully explained with reference to this model in respect to C1' hydrogens. The planes of base pairs are indicated by the diagonal lines.

observed for 2'-, 2''-, and 3'-hydrogen resonances. This is evidence for the dye binding in the minor, rather than the major, groove of the oligonucleotide. A full explanation for the differences induced in C1'H chemical shifts along the length of the oligonucleotide chain can be obtained by reference to a model of the complex when Hoechst 33258 is bound to the AATT region of the duplex. The significant point about the chemical shift differences is that resonances moved to lower frequency (i.e., resonances especially from hydrogens at T^7 and T^8 positions on both strands of DNA are strongly shielded). Indeed shielding occurs to such an extent that the biggest chemical shift difference is over 1 ppm. This indicates that T^7 and T^8 C1' hydrogens are strongly influenced by diamagnetic anisotropy, the sources of which must be the two benzimidazole moieties of the dye. As shown in Figure 11, the phenol ring also influences the chemical shift of the C^9 C1' hydrogen for the same reason. In the case of A^8 and A^6, the C1' hydrogens lie above the piperazine ring, which does not affect chemical shift in anything like the dramatic way of the benzimidazole rings. Thus, chemical shift measurements not only show the dye to bind in the minor groove of d-$(CGCGAATTCGCG)_2$ but also provide strong evidence for binding at the central AATT site.

(ii) Evidence from Intermolecular nOes. nOes between Hoechst 33258 and the oligonucleotide d-(CGCGAATTCGCG) confirm that the dye is indeed binding at the central AATT site, in the minor groove. The exchangeable N4 and N3 hydrogens of the dye show nOes to hydrogens in the oligonucleotide that lie on the floor of the minor groove. Specifically, N1H shows an nOe to $A^{6'}$ C2H, and N3H shows an nOe to A^6 C2H. In addition, the Hoechst methyl group shows an nOe to A^5 C2H, also on the minor groove floor. Together with the additional nOes shown in Table III (Figure 10), computer graphics shows that the nOes are only consistent with a complex formed at the central AATT site.

Evidence for a Single Binding Site. In the 1:1 complex only one set of resonances exists for the dye. Since the dye is in slow exchange with the DNA, these resonances represent a single form, rather than an average of several forms interconverting rapidly on the NMR timescale.

In addition, the two sets of resonances for the DNA are the result of two strands with different identities within the *same* molecule, rather than two different molecules interconverting. This underlies the fact that the NMR spectrum represents a single mode of binding. The cross-peaks between Hoechst N1H and N3H resonances and $A^6/A^{6'}$ C2H resonances illustrate this. Thus, N1H shows a cross-peak to $A^{6'}$ C2H but not to A^6 C2H. Similarly, N3H shows a cross-peak to A^6 C2H but not to $A^{6'}$ C2H. No exchange cross-peaks are observed between N1H and A^6 C2H or between N3H and A6' C2H, a result of the fast chemical exchange undergone by the free-Hoechst exchangeable hydrogens. The rate of chemical exchange of the N–H on the dye is faster than the rate of reorientation of the dye at its minor-groove binding site. This leads to a unique nOe for the dye NH to only one of the two A^6 C2H protons that are, in principle, accessible to it prior to binding. This allows total confidence in site identification from such nOe data. Thus, the dye, when it comes off the complex and reorients itself, goes back into the minor groove at the same binding site, even though it may have turned through 180°. The result of this is that the NMR spectrum can be taken to represent an essentially static model. Whichever "direction" the drug binds in, the same complex is formed in these solution NMR studies.

Comparison with Other Minor-Groove Ligand NMR Studies. Signal doubling of oligonucleotide resonances, arising from lifting of diad symmetry on ligand binding, has been reported for lexitropsins by Lee et al. (1988a,b). In one of these cases, spin diffusion was asserted to be the reason for the appearance of very few COSY and NOESY cross-peaks (Lee et al., 1988a). In addition, only one of three possible cytosine CH5–CH6 cross-peaks was detected. This was ascribed to high local mobility of cytosine, a feature to which the intensity of the CH5–CH6 correlation is reported as very sensitive (Borah et al., 1985). In both of these studies (Lee et al., 1988a,b) insufficient cross-peak data were available to assign all of the protons of the oligonucleotide in the complex with the appropriate lexitropsin. In the present study, a wealth of nOe cross-peak detail is present. This makes the Hoechst 33258–oligonucleotide system an excellent model system for NMR study of fine details of mutual recognition between minor-groove ligand and its binding site on DNA.

Resonance doubling has been reported (Patel & Shapiro, 1986) when netropsin binds to the minor groove of the duplex of d(GGAATTCC) but again only a relatively small number of resonances were affected relative to the Hoechst 33258–d$(CGCGAATTCGCG)_2$ case. The nOe cross-peak data could be interpreted in terms of netropsin binding to the minor groove in the AATT site of the duplex and showed that there was no room for water molecules between the floor of the minor groove and the drug. This is also the case for Hoechst 33258 in the present study and for (4*S*)-(+)-anthelvencin A binding to d$(CGCAATTGCG)_2$ for which an NMR study indicating nOe contacts between drug and the central AATT region has been presented (Lee et al., 1989).

Protonation State of Bound Ligand. It has been suggested (Teng et al., 1988) that the pK_a values of the benzimidazole sites of Hoechst 33258 will be approximately 5.48, presumably based on comparisons with literature data for benzimidazole itself as a model. It is not clear that the pK_a was actually measured for Hoechst 33258. It is not safe to assume, given this low pK_a for the benzimidazolium proton(s), that the ligand must bind necessarily in its monoprotonated state (i.e., with net charge of +1), with neutral benzimidazole sites. The energy required to alter a pK_a by 1 unit is approximately 1.4 kcal·mol^{-1} at 25 °C (Douglas, 1976). By binding in the benzimidazolium protonated state, energy would have to be expended to raise the p*K* value(s). However, this having been done, added stabilization of the imidazolium states would be provided by the marked negative electrostatic potential of the minor groove, predominant especially in AATT-rich regions, as occupied in this case. Moreover, such electrostatic stabilization would be augmented relative to free, aqueous solution by the lowering of the dielectric constant from the bulk solvent

value of 80 D to ≈20 D as has been determined for the minor-groove/Hoechst 33258 interface (Jin & Breslauer, 1988). At present we cannot assess from our NMR results whether the dye is bound with one or both benzimidazole sites in their protonated states. This aspect is being pursued.

In this context we are also studying the dynamics of the complex and on/off rates are being determined along with local rotational freedom, e.g., potential ring flip by the phenolic moiety of the ligand.

Conclusion

From this NMR spectroscopic study we can confirm that in solution Hoechst 33258 binds tightly to d-$(CGCGAATTCGCG)_2$ through the minor groove. Our data are consistent with the crystal structure interpretation offered by Teng et al. (1988), with binding determinants being provided by the central AATT stretch of residues. The propellor twisting reported by Teng et al. (1988) for the bound ligand's planar aromatic rings is identified in our study by analysis of the nOe contacts that require such orientation. The nOe contacts determined can be compared with the (heteronuclear) distances given in Table I of Teng et al. and several of them match up within the experimental limitations of nOe intensity estimation. The snug fit of Hoechst 33258 to the minor groove, shown (in Figure 10) by molecular modeling based on nOe data, clearly indicates that water must be excluded from the minor groove in binding. This results in a lowered local dielectric constant within the interface region between the oligonucleotide minor groove and the bound surface of Hoechst 33258 [see Jin and Breslauer (1988)]. The implications of this for the pK_a values of the bound ligand are that it may be energetically worthwhile for the ligand benzimidazole pK_a values to be raised to benefit from this and the negative electrostatic potential of the AATT region.

Added in Proof

A high-field NMR study of Hoechst 33258 in a 2:1 complex with $d(CTTTTGCAAAAG)_2$ has been published recently (Searle & Embrey, 1990).

Acknowledgments

We are grateful to the SERC and MRC for use of the high-field NMR facilities at the University of Leicester and Mill Hill, respectively.

Registry No. Hoechst 33258, 23491-45-4; d(CGCGAATTCGCG), 77889-82-8.

References

Anderson, W. F., Ohlendorf, D. H., Takeda, Y., & Matthews, B. W. (1981) *Nature (London) 290*, 754–758.

Aue, W. P., Bartholdi, E., & Ernst, R. R. (1976) *J. Chem. Phys. 64*, 2229–2246.

Baguley, B. (1982) *Mol. Cell. Biochem. 43*, 167–181.

Bontemps, J., Houssier, C., & Fredericq, E. (1975) *Nucleic Acids Res. 2*, 971–984.

Borah, B., Roy, S., Zon, G., & Cohen, J. S. (1985) *Biochem. Biophys. Res. Commun. 133*, 380–388.

Dervan, P. B. (1986) *Science (Washington, D.C.) 232*, 464–471.

Douglas, K. T. (1976) *Prog. Bioorg. Chem. 4*, 193–238.

Dreyer, G. B., & Dervan, P. B. (1985) *Proc. Natl. Acad. Sci. U.S.A. 82*, 968–972.

Goodsall, D., & Dickerson, R. E. (1986) *J. Med. Chem. 29*, 727–733.

Hare, D. R., Wemmer, D. E., Chan, S.-H. Drobny, G., & Reid, B. R. (1983) *J. Mol. Biol. 171*, 319–336.

Harshman, K. D., & Dervan, P. B. (1985) *Nucleic Acids Res. 13*, 4825–4835.

Hore, P. J. (1983a) *J. Magn. Reson. 54*, 539–542.

Hore, P. J. (1983b) *J. Magn. Reson. 55*, 283–300.

Jeener, J., Meier, B. H., Backmann, P., & Ernst, R. R. (1979) *J. Chem. Phys. 71*, 4546–4553.

Jin, R., & Breslauer, K. J. (1988) *Proc. Natl. Acad. Sci. U.S.A. 85*, 8939–8942.

John, D. C. A., & Douglas, K. T. (1989) *Biochem. Biophys. Res. Commun. 165*, 1235–1242.

Kissinger, K., Krowicki, K., Dabriowak, J. C., & Lown, J. W. (1987) *Biochemistry 26*, 5590–5595.

Lee, M., Hartley, J. A., Pon, R. T., Krowicki, K., & Lown, J. W. (1988a) *Nucleic Acids Res. 16*, 665–684.

Lee, M., Chang, D.-K., Hartley, J. A., Pon, R. T., Krowicki, K., & Lown, J. W. (1988b) *Biochemistry 27*, 445–455.

Lee, M., Shea, R. G., Hartley, J. A., Kissinger, K., Pon, R. T., Vesnaver, G., Breslauer, K. J., Dabriowak, J. C., & Lown, J. W. (1989) *J. Am. Chem. Soc. 111*, 345–354.

Leupin, W., Chazin, W. J., Hyberts, S., Denny, W., & Wüthrich, K. (1986) *Biochemistry 25*, 5902–5910.

Lown, J. W., Sondhi, S. M., Ong, C.-W., Skorobogaty, A., Kishikawa, H., & Dabriowak, J. C. (1986) *Biochemistry 25*, 5111–7.

Macura, S., Huang, Y., Suter, D., & Ernst, R. R. (1981) *J. Magn. Reson. 43*, 259–281.

Marion, D., & Wüthrich, K. (1983) *Biochem. Biophys. Res. Commun. 113*, 967–974.

Nagayama, K., Kumar, A., Wüthrich, K., & Ernst, R. R. (1980) *J. Magn. Reson. 40*, 321–334.

Neidle, S., Pearl, L. H., & Skelly, J. V. (1987) *Biochem. J. 243*, 1–13.

Parkinson, J. A., Barber, J., Douglas, K. T., Rosamund, J., & Sharpless, D. (1989) *J. Chem. Soc., Chem. Commun.*, 1023–1025.

Patel, D. J., & Shapiro, L. (1985) *Biochimie 67*, 887–915.

Patel, D. J., & Shapiro, L. (1986a) *Biopolymers 25*, 707–727.

Patel, D. J., & Shapiro, L. (1986b) *J. Biol. Chem. 261*, 1230–40.

Patel, D. J., Shapiro, L., & Hare, D. R. (1987) *Annu. Rev. Biophys. Biophys. Chem. 16*, 423–454.

Pjura, P. E., Grzeskowiak, K., & Dickerson, R. E. (1987) *J. Mol. Biol. 197*, 257–271.

Rajagopal, P., Gilbert, D. E., van der Marel, G. A., van Boom, J. H., and Feigon, J. (1988) *J. Magn. Reson. 78*, 526–537.

Reed, C. J., & Douglas, K. T. (1989) *Biochem. Biophys. Res. Commun. 162*, 1111–1117.

Reid, B. R. (1987) *Q. Rev. Biophys. 20*, 1–34.

Ridler, P. J., & Jennings, B. R. (1980) *Int. J. Biol. Macromol. 2*, 313–317.

Searle, M. S., & Embrey, K. J. (1990) *Nucleic Acids Res. 18*, 3753–3767.

Segel, I. H. (1975) *Enzyme Kinetics*, p 218, Wiley-Interscience, New York.

Sigman, D. S. (1986) *Acc. Chem. Res. 19*, 180–186.

Stokke, T., & Steen, H. B. (1985) *J. Histochem. Cytochem. 33*, 333–338.

Teng, M.-K., Usman, N., Frederick, C. A., & Wang, A. H.-J. (1988) *Nucleic Acids Res. 16*, 2671–90.

Wang, J.-H. (1986) *Nature (London) 319*, 183–184.

Zakrzewska, K., & Pullman, B. (1988) *J. Biomol. Struct. Dyn. 5*, 1043–1058.

Zimmer, Ch., & Wahnert, U. (1986) *Prog. Biophys. Mol. Biol. 47*, 31.